BASIC SCIENCE

Longitudinal outcomes of circumlimbal suture model-induced chronic ocular hypertension in Sprague-Dawley albino rats

Yamunadevi Lakshmanan[1] · Francisca Siu Yin Wong[1] · Bing Zuo[2] · Bang Viet Bui[3] · Henry Ho-Lung Chan[1,2] (ID)

Abstract

Purpose To characterise longitudinal structural and functional changes in albino Sprague-Dawley rats following circumlimbal suture ocular hypertension (OHT) induction.

Methods Ten-week-old rats ($n = 24$) underwent suture implantation around the limbal region in both eyes. On the next day, the suture was removed from one eye (control eyes) and left intact in the other eye (OHT eyes) of each animal. Intraocular pressure (IOP) was monitored weekly twice for the next 15 weeks. Optical coherence tomography (OCT) and electroretinogram (ERG) were measured at baseline and weeks 4, 8, 12, and 15, and eyes were then collected for histological assessment.

Results Sutured eyes ($n = 12$) developed IOP elevation of ~50% in the first 2 weeks that was sustained at ~25% above the control eye up to week 15 ($p = 0.001$). Animals with insufficient IOP elevation ($n = 6$), corneal changes ($n = 3$), and attrition ($n = 3$) were excluded from the analysis. OHT eyes developed significant retinal nerve fibre layer (RNFL) thinning (week 4: $-19 \pm 14\%$, $p = 0.10$; week 8: $-17 \pm 12\%$, $p = 0.04$; week 12: $-16 \pm 10\%$, $p = 0.04$, relative to baseline) and reduction in retinal ganglion cell (RGC) density ($-32 \pm 26\%$, $p = 0.02$). At week 15, both inner ($9 \pm 7\%$, $p = 0.01$) and outer retinal layer thicknesses ($6.0 \pm 5\%$, $p = 0.001$) showed a mild increase in thicknesses. The positive scotopic threshold response ($-28 \pm 25\%$, $p = 0.04$) and a-wave were significantly reduced at week 12 ($-35 \pm 21\%$; $p = 0.04$), whereas b-wave was not significantly affected (week 12: $-18 \pm 27\%$, $p = 0.24$).

Conclusion The circumlimbal suture model produced a chronic, moderate IOP elevation in an albino strain that led to RNFL thinning and reduced RGC density along with the reductions in ganglion and photoreceptoral cell functions. There was a small thickening in both outer and inner retinal layers.

Keywords Glaucoma · Intraocular pressure · Ocular hypertension · Animal model · Circumlimbal suture · Albino rat

Introduction

Glaucoma is a blinding disease which is predicted to affect 76 million people worldwide by 2020 [1], with 11.2 million

✉ Henry Ho-Lung Chan
  henryhl.chan@polyu.edu.hk

[1] Laboratory of Experimental Optometry (Neuroscience), School of Optometry, The Hong Kong Polytechnic University, Hong Kong SAR China

[2] Centre for Myopia Research, School of Optometry, The Hong Kong Polytechnic University, Hong Kong SAR China

[3] Department of Optometry and Vision Sciences, University of Melbourne, Melbourne Australia

people presenting with bilateral blindness [2]. Increased intraocular pressure (IOP) is the major risk factor and the only modifiable factor in the current management of glaucoma [3, 4]. While IOP lowering delays disease progression, some patients continue to show vision loss despite well-controlled IOP [3–5]. Thus, there remains a need to better understanding the pathogenesis of glaucoma. In this respect, animal models of glaucoma provide a means to study the disease mechanisms as well as to test novel treatment approaches.

Various animal models have been developed for studying glaucoma, including those in non-human primates, dogs, rodents, zebra fish, rabbits, sheep, cows, and birds [6]. Rodents are currently in wide-spread use due to their low cost, effortless handling, ease of IOP measurement in awake animals, and availability of various approaches to induce ocular hypertension (OHT) [7]. To simulate closed- and open-angle glaucoma types, OHT models aim to obstruct aqueous outflow either at, before, or after the trabecular meshwork [8]. This

can be achieved via intracameral injection of materials (e.g. microbeads) into the anterior chamber [9–11], laser photocoagulation of the trabecular meshwork [12–14] and/or limbal episcleral veins [15, 16], injection of hypertonic saline into episcleral vein [17], and cauterisation of episcleral veins [18]. Such models mimic certain aspects of glaucoma and are generally reproducible in rodents; however, each has its own limitations. Thus, factors to consider when choosing a model of glaucoma include the invasiveness of the procedure, the need for repeated interventions, the presence of excessive secondary inflammation and anterior segment changes that impact imaging, and whether there is a need for specialised instruments or training.

Recently, a circumlimbal suture model was developed to induce chronic OHT in rodents [19]. It is a simple and inexpensive approach that can be applied as a single intervention and facilitates longitudinal structural and functional assessments. In addition, the model allows lowering of IOP possible by simply removing the suture at different time points, which assists in studying the recovery of neuronal dysfunction or structural preservation [20, 21]. While this model was well characterised in pigmented strains [19, 22, 23], the effect of suture-induced chronic IOP elevation in albino rat strains remains unknown. Albino rats are often used for OHT model induction to study the effect of IOP elevation on neuronal degeneration [9, 12, 14, 16, 18, 24–26] and to test the efficacy of IOP lowering or neuroprotective therapies on retinal ganglion cell (RGC) survival [15, 27–31]. Previously, two independent studies from the same laboratory revealed that suture model induction in albino CD-1 mice [32] could develop only moderate IOP elevation (∼30%) sustaining for 2 weeks as compared with C57-pigmented mice [22] that produced relatively higher magnitude of IOP elevation (∼70%) for 12 weeks. Despite moderate and brief period of IOP elevation, CD-1 developed retinal nerve fibre layer (RNFL) thinning earlier than C57 mice. Thus, we hypothesise that the circumlimbal suture model induction in albino rat strain may exhibit differential outcomes in terms of magnitude of IOP elevation, onset of retinal structure-function changes, and its rate of progression. In this study, we sought to use a Sprague-Dawley albino rat strain to investigate the effect of circumlimbal suture-induced chronic IOP elevation on longitudinal retinal structure using in vivo optical coherence tomography (OCT) imaging and histology, and functional changes by electroretinogram (ERG).

Materials and methods

Animals

Adult albino female Sprague-Dawley (SD) rats of 10 weeks old (180–210 g) were housed in 12:12 light/dark cycle lighting environment (200 lx maximum). Food (PicoLab® diet 20 (5053), PMI Nutrition International, Richmond, IN, USA) and water were available ad libitum. All experimental procedures and care involving the animals adhered to the ARVO Statement for the Use of Animals in Ophthalmic and Vision Research. The study was approved by The Animal Ethics Sub-Committee of The Hong Kong Polytechnic University.

Experimental design and OHT induction

Twenty-four 10-week-old SD rats underwent OHT induction. Following baseline ERG and OCT measurements, all animals were acclimatised for 3 days to awake IOP measurements using a rebound tonometer (Tonolab, Icare, Vantaa, Finland). Baseline IOP was determined by averaging IOP measurements collected on two subsequent days. Each IOP measurement was average of 5 reliable readings, and the measurements were taken between 10:30 AM to 12:30 PM to avoid diurnal variations. On the day of OHT induction, animals were anesthetised with a mixture of 60-mg/kg ketamine and 5-mg/kg xylazine (Alfasan International B.V, Woerden, Holland) via intraperitoneal injection. Following the application of a drop of topical anaesthetic (Provain-POS 0.5% *w/v* eye drop; URSAPHARM, Saarbrücken, Germany), both eyes underwent suture application. A suture (8/0 nylon) was applied around the globe at approximately 1.5–2 mm behind the limbus. The suture was secured using 6 to 7 subconjunctival anchor points as reported [19], with care taken to avoid the compression of the major episcleral veins. The suture was then tightened with a slipknot until IOP reached 60–70 mmHg. The leftover suture was trimmed to prevent it from rubbing against the cornea. Eyes were then treated with a topical antibiotic eye drops, gentamicin (Gibco, Thermo-Fisher Scientific, Waltham, MA, USA). To prevent the corneal dehydration during recovery from anaesthesia, lacryvisc gel (Alcon, Rueil-Malmaison, France) was applied.

At post-operative day one, the suture was removed from one eye (control) and left intact in the other randomly chosen eye (suture). IOP was monitored on alternate days for the first week and twice a week thereafter until week 15. Sutured eyes that maintained an IOP elevation of 25% above their fellow control eyes (suture removed) during the first week were considered to be successful (OHT eye) and were followed up till week 15. OCT imaging and ERG assessment were undertaken at 4, 8, 12, and 15 weeks after OHT induction. The changes in the retinal structure and function in the OHT eyes relative to the control eyes were determined. To ascertain that the changes in OHT eyes were mainly induced by chronic IOP elevation instead of the initial IOP spike observed, a similar duration of IOP spike was induced in the control eyes by leaving the suture intact for a day. As animals

required sedation for suture removal, the procedure was scheduled on the next day to avoid repeated anaesthesia within the same day.

Animals that had insufficient IOP elevation ($n = 6$; less than 25% of fellow eye) in the first 2 weeks of OHT induction were not further assessed. Moreover, animals that developed corneal changes ($n = 3$; 12%) and attrition ($n = 3$, 12% of rats failed to recover from general anaesthesia during ERG/OCT measurements) were excluded from final analysis. Twelve rats completed the study and were sacrificed to collect retinal samples for morphological examination at week 15.

Optical coherence tomography

Spectral domain OCT (SD-OCT) (Micron IV, Phoenix Research Lab, Pleasanton, CA, USA) was used to image the peripapillary retina. OCT imaging and analysis were conducted as described in our previous study [33]. Briefly, following ketamine-xylazine anaesthesia, the pupils were dilated using Mydriacyl 1% eye drops (Alcon-Couvreue, Puurs, Belgium). Lubricating gel was applied on the corneal surface to improve the contact between the eye and the objective lens. A circular B-scan with a radius of 0.51 mm, consisting of 1024 A-scans, was used to image the retinal layers. The axial and transverse resolutions of these images were 1.8 μm and 3.0 μm respectively. Semi-automated segmentation algorithm (Insight software, Phoenix Research Lab) was applied to analyse the B-scan images to provide total retinal thickness (TRT), retinal nerve fibre layer thickness (RNFLT), inner retinal layer thickness (IRLT), and outer retinal layer thickness (ORLT). The TRT was measured from the retinal pigment epithelium (RPE) layer to the inner limiting membrane, the IRLT included the thicknesses of the inner plexiform and inner nuclear layer, and the ORLT was measured from the RPE to the outer plexiform layer. The mean thickness of each layer was determined by averaging 1024 data points that covered the circumference of the circle.

Electroretinography

The full-field electroretinogram was recorded using a white LED light (Ganzfeld, Q450; RETI Animal, Roland Consult, Brandenburg an der Havel, Germany). ERG measurements and analyses were conducted as described in our earlier report [33]. Briefly, animals were dark adapted overnight for 12 h and were anesthetised (ketamine-xylazine mixture) prior to data acquisition. Eyes were dilated and a drop of lubricating gel was applied to prevent corneal drying. Responses were obtained using gold ring electrodes placed on the corneal surface of both eyes; needle electrodes inserted into the lateral canthi and base of the tail served as reference and ground electrodes, respectively. As chronic IOP elevation largely affects the RGCs, the positive scotopic threshold response (pSTR) was recorded as a surrogate measure for RGC functions [34] along with the traditional recording of mixed scotopic responses (a- and b-waves). The pSTR was recorded using a series of brief flash (pulse length of 2 μs) stimulation intensities ranging from − 4.8 to − 4.05 log cd s/m^2 in 0.15-log cd s/m^2 steps. Each stimuli response was the average of 30 responses with an inter-stimulus interval of 2 s. Scotopic (mixed rod and cone) responses were recorded using a single flash of 1.3 log cd s/m^2. All signals were recorded with a band pass filter of 0.1–1000 Hz. The amplitudes and implicit time of pSTR, scotopic a-wave, and b-wave responses were quantified.

Retinal histology

After OCT and ERG measurements at week 15, animals were euthanised by CO_2 asphyxiation. The eye cups were collected and fixed overnight using 4% paraformaldehyde in PBS at room temperature. The tissues were dehydrated using graded ethanol and paraffin embedded. Five-micrometre sections parallel to the optic nerve were collected, stained with haematoxylin and eosin (H&E), and imaged using a light microscope at × 200 magnification (Nikon, Tokyo, Japan). Regions of 500 μm × 500 μm of the central (250 μm away from the scleral canal opening) and peripheral retina (250 μm away from the ora serrata) as well as the anterior angle and optic nerve head were selected for morphological analysis. Cell density in ganglion cell layer (GCL) (cells/mm) was calculated by manually counting the number of nuclei in the ganglion cell layer and divided it by the corresponding retinal length measured using ImageJ (National Institute of Health, Bathesda, MA, USA) as reported previously [33].

Retina immunohistochemistry

The retinal sections were de-paraffinised, blocked with serum, and incubated with primary mouse anti-β-III-tubulin (1:1000, BioLegend, San Diego, CA, USA) at 4 °C overnight. To visualise the signal, the retinal sections were then incubated with Alexa Fluor 488 goat anti-mouse IgG (1:500; Molecular Probes, Invitrogen, Carlsbad, CA, USA) and the cell nuclei were counter-stained with 4′-6-diamidino-2-phenylindole (DAPI). A light microscope (Nikon, Tokyo, Japan) was used to image the stained sections at × 200 magnification. The β-III-tubulin positive cells from central retinal region of 500 μm × 500 μm were manually counted and divided by the corresponding retinal length using ImageJ (National Institute of Health, Bathesda, MA, USA) to return the RGC density (cells/mm) [35].

Statistical analysis

All analyses were performed using SPSS 23 (IBM Corp, Armonk, NY, USA). Data were normally distributed and thus presented as mean with standard deviation. Two-way repeated measures (RM) ANOVA was used to compare differences in IOP, OCT, and ERG parameters between suture and fellow control eyes that were measured over time (baseline, post-OHT induction weeks 4, 8, 12 and 15) with Bonferroni post hoc correction. For cell density in GCL, a paired t test was used to compare the difference between suture and fellow control eyes. Also, the rates of change in structural and functional parameters upon OHT induction in the suture eye were first expressed relative to their fellow control eye ((suture-control)/control $\times 100$) and then as a difference (%) from baseline [35]. The level of significance was set as $p < 0.05$.

Results

Circumlimbal suture model produced a moderate IOP elevation in SD rats

Figure 1a shows an illustration of circumlimbal suture secured around the rat eye. Figure 1b shows the position of suture from one representative rat on the day of suture placement (day 0) and at post-operative weeks 4, 8, and 15. Twelve animals met the $\geq 25\%$ criteria for IOP elevation throughout the 15 weeks and were free of complications. Baseline IOP in sutured and fellow control eyes was 11 ± 1 mmHg. Immediately after securing the suture, IOP spiked to 64 ± 16 mmHg. This changed the iris colour from red to pale red. After 5 min of suture

placement, IOP returned to 40 ± 15 mmHg and the iris regained its red colour.

Figure 1c shows that IOP in sutured eyes was significantly greater than fellow control eyes (two-way RM ANOVA: between eyes: $p = 0.001$; interaction effect: $p = 0.003$). Post hoc analysis shows that this was significant for all weeks, except for weeks 9 ($p = 0.07$) and 14 ($p = 0.09$). The sutured eyes developed an IOP elevation of $\sim 50\%$ greater than the fellow control eye during the first 2 weeks of the study period (control: 12 ± 1 mmHg; suture: 18 ± 4 mmHg, $p < 0.001$). Subsequently, the IOP was maintained at $\sim 25\%$ increase till the end of the study at week 15. Suture placement for 1 day in the control eyes did not affect the IOP levels over the next 15 weeks, which remained similar to baseline.

Effect of IOP elevation on OCT-measured retinal layers thicknesses

Figure 2 illustrates segmented SD-OCT B-scans along with fundus photographs from a representative rat showing the longitudinal changes in sutured (Fig. 2a) and fellow control eyes (Fig. 2b) from baseline to week 15. All layers including TRT, RNFLT, IRLT, and ORLT showed a significant interaction between eyes over time (two-way RM ANOVA: interaction: $p = 0.001$). Baseline TRT was similar between eyes ($p = 0.90$). Following suture placement, TRT showed a slight thinning at week 4 ($-1.6 \pm 2.3\%$, $p = 0.03$) when compared with fellow control eyes. At week 12 ($2.0 \pm 2.9\%$, $p = 0.04$) and week 15 ($5.0 \pm 4.7\%$, $p = 0.001$), TRT in sutured eyes was slightly thicker than fellow control eyes (Fig. 3a).

The RNFL in sutured eyes (Fig. 3b) was significantly thinner than that in fellow control eyes at weeks 4 ($p = 0.03$), 8 ($p = 0.03$), and 12 ($p = 0.04$). The rate of RNFLT loss (Fig. 6a)

Fig. 1 Chronic OHT induction was achieved by securing a suture firmly around the globe. **a** An illustration of circumlimbal suture secured at a distance of ~ 1.5 to 2 mm behind the limbus in the rat eye. **b** Suture positions from one representative rat at day 0 (10 min after suture placement) and end of weeks 4, 8, and 15 (white arrow). **c** The circumlimbal suture induced a moderate and chronic IOP elevation in albino rats ($n = 12$) for at least 15 weeks, while control eyes which had the suture removed at day 1 showed stable IOP. Error bars: standard deviation. *$p < 0.05$ (*Bonferroni's post hoc test of two-way RM ANOVA)
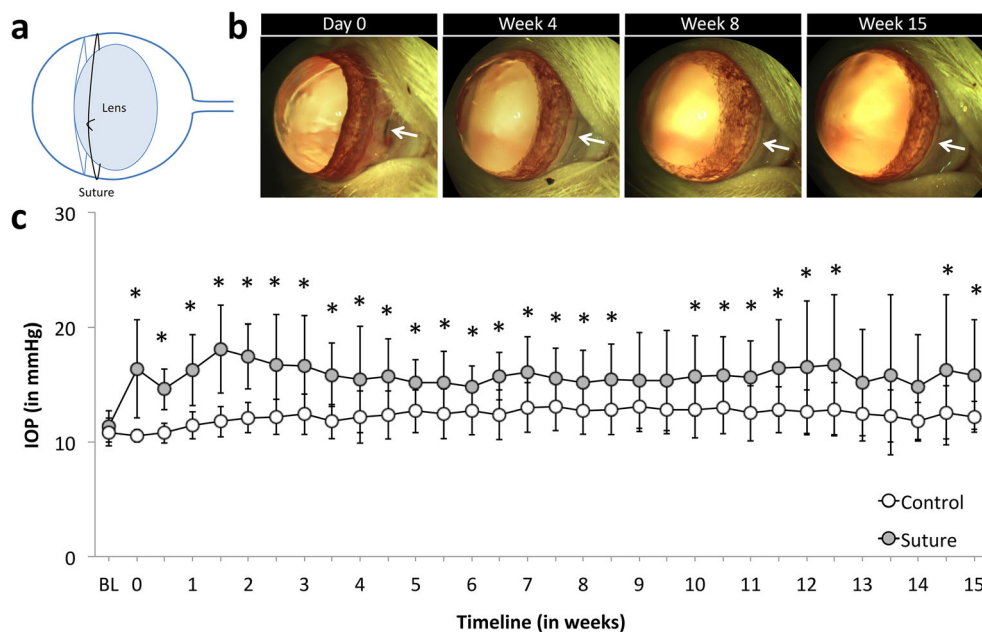
Fig. 2 Peripapillary SD-OCT B-scan images and fundus photographs of **a** sutured eye and **b** fellow control of one representative rat taken at baseline, and after 4 and 15 weeks of IOP elevation. OCT circle scan positions are indicated in black circle on their corresponding fundus photographs. OCT images were segmented to determine RNFL, IRL, and ORL thicknesses. RNFL, retinal nerve fibre layer; IRL, inner retinal layer (includes inner plexiform and inner nuclear layer); ORL, outer retinal layer (from RPE to outer plexiform layer)
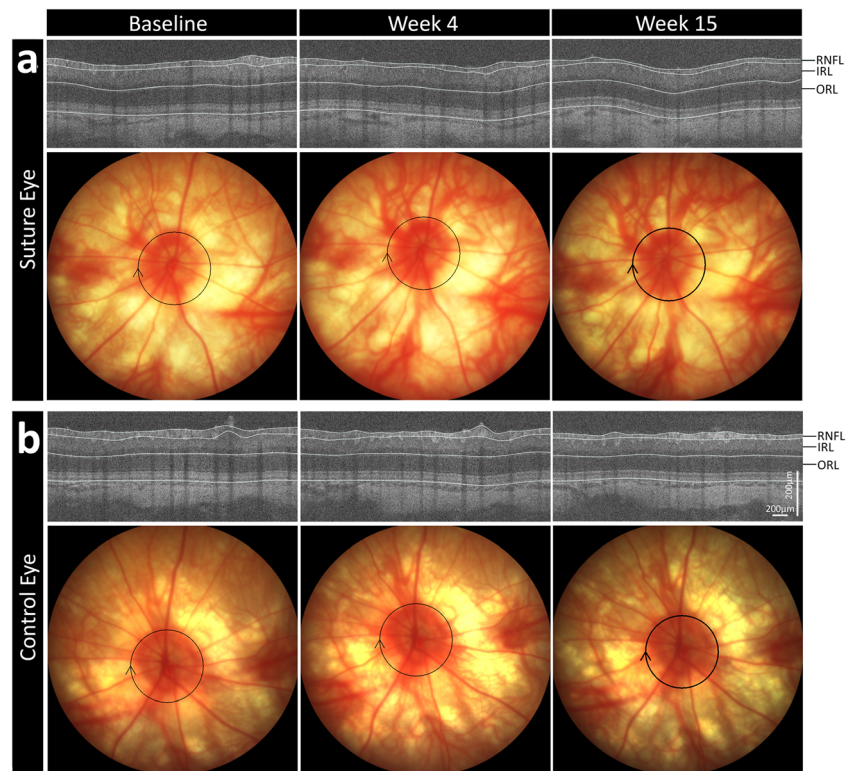
at week 4 was $-19 \pm 14\%$ of fellow control ($p = 0.10$). Significant loss was detected at weeks 8 ($-17 \pm 12\%$, $p = 0.04$) and 12 ($-16 \pm 10\%$, p = 0.04). As for IRLT and ORLT, both were similar in suture and control eyes at week 4, but were significantly thicker ($p < 0.05$) in sutured eyes from week 8 to the end of the study (Fig. 3c and d). At week 15, the IRLT and ORLT in sutured eyes were $9 \pm 7\%$ ($p = 0.01$) and $6 \pm 5\%$ ($p = 0.001$) thicker than the fellow control eyes, respectively.

Effect of IOP elevation on ERG-measured retinal functions

Figure 4 shows averaged pSTR and scotopic ERG traces of suture eyes compared with fellow control eyes. The pSTR responses (Fig. 5a) of sutured eyes were significantly reduced at week 12 ($p = 0.04$) with no further reduction at week 15 (two-way RM ANOVA: between eyes: $p = 0.27$; time effect: $p = 0.01$; interaction: $p = 0.07$). Scotopic b-wave responses (Fig. 5b) were not significantly different between sutured and control eyes (two-way RM ANOVA: between eyes: $p = 0.52$; time effect: $p = 0.65$; interaction: $p = 0.35$). Similar to the pSTR, scotopic a-wave responses (Fig. 5c) of the suture eye dropped significantly at week 12 (p = 0.01) with no further reduction at week 15 (two-way RM ANOVA: between eyes: $p = 0.06$; time effect: $p = 0.48$; interaction: $p = 0.05$). The inner retinal (pSTR), mid-retinal (b-wave), and outer retinal (a-wave) functional loss at week 12 were $-28 \pm 25\%$,

($p = 0.04$), $-18 \pm 27\%$ ($p = 0.24$), and $-35 \pm 21\%$ ($p = 0.04$) respectively.

Table 1 gives the implicit time of pSTR, b-wave, and a-wave responses of sutured and fellow control eyes. There was no difference in pSTR implicit time between suture and fellow control eyes at all time points (two-way RM ANOVA: between eyes: $p = 0.09$; time effect: $p = 0.38$; interaction: $p = 0.63$). However, the scotopic b-wave (two-way RM ANOVA: between eyes: $p = 0.05$; time effect: $p = 0.10$; interaction: $p = 0.82$) and a-wave (two-way RM ANOVA: between eyes: $p = 0.03$; time effect: $p = 0.59$; interaction: $p = 0.03$) in sutured eyes were delayed at weeks 8 (b-wave: control: 69.9 ms, suture: 74.1 ms, $p = 0.03$) and 12 (a-wave: control: 7.7 ms, suture: 8.2 ms, $p = 0.01$), respectively.

A summary of the effects of IOP elevation on retinal structure (thicknesses of RNFL, IRL, and ORL) and function (pSTR, scotopic b-wave, and a-wave responses) is shown in Fig. 6a and b, respectively.

Effect of IOP elevation on GCL density and axonal arrangements

Figure 7 presents the H&E-stained retinal cross-section that shows no obvious change in retinal layers at both peripheral and central regions from a representative sutured (Fig. 7b and d) and its fellow control eyes (Fig. 7a and c) at week 15. Quantification revealed that the cell density in the GCL in suture eyes was significantly reduced in both peripheral ($-$
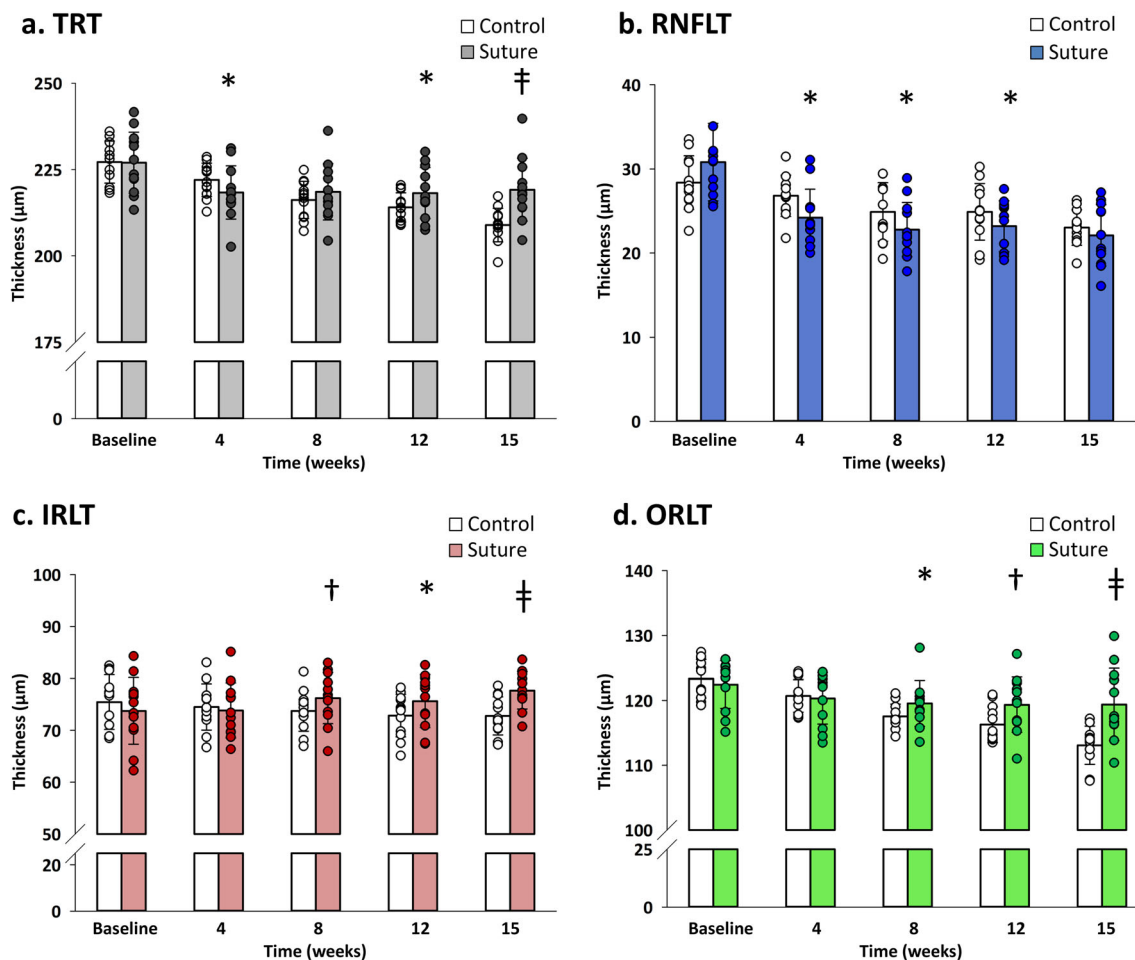
Fig. 3 The effect of chronic IOP on OCT-measured retinal thicknesses. The thicknesses of **a** TRT, **b** RNFLT, **c** IRLT, and **d** ORLT were compared between sutured and fellow control eyes ($n = 12$). $*p < 0.05$; $^{†}p < 0.01$; $^{‡}p < 0.001$ ($*,^{†,‡}$Bonferroni's post hoc test of two-way RM ANOVA). Error bars: standard deviation. Each circle in the bar chart represents individual data points of the animals. TRT, total retinal thickness; RNFLT, retinal nerve fibre layer thickness; IRLT, inner retinal layer thickness; ORLT, outer retinal layer thickness

$18 \pm 16\%$, $p = 0.02$) and central ($-16 \pm 12\%$, $p = 0.02$) retina as compared with fellow control eyes (Fig. 7e). Considering the presence of both RGC and amacrine cells in the GCL, the

retinal sections were further stained with β-III-tubulin, a RGC-specific marker. The RGC density determined from the central retina showed a significant reduction in the suture
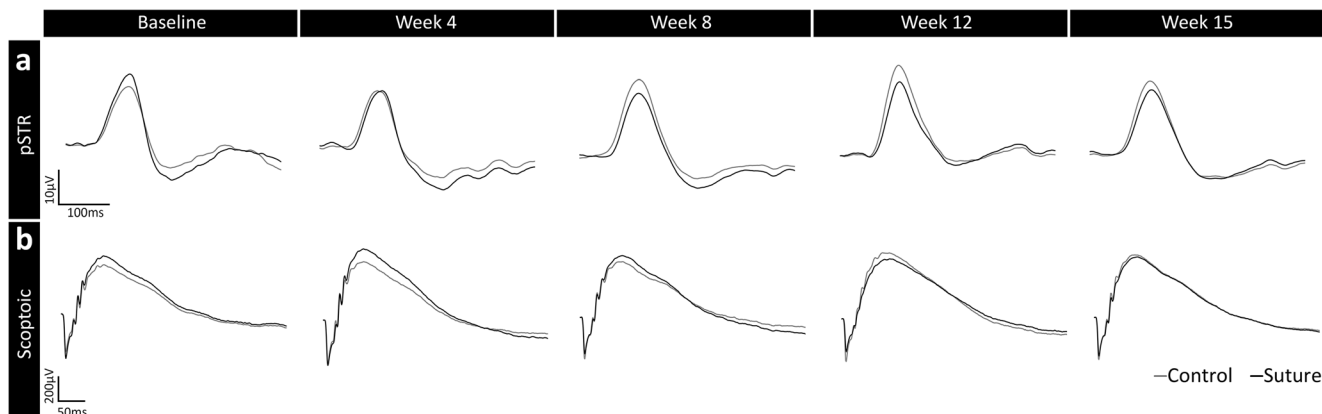
Fig. 4 Changes in inner and outer retinal responses over the 15 weeks of IOP elevation. **a** pSTR and **b** scotopic ERG. Black and grey traces represent averaged responses from suture and control eyes ($n = 12$) respectively

Fig. 5 The effect of chronic IOP on ERG-measured retinal functions. The responses of ganglion, bipolar, and photoreceptor cell responses were presented as **a** pSTR, **b** b-wave, and **c** a-wave respectively ($n = 12$). Error bars: standard deviation. Each circle in the bar chart represents individual data points of the animals. $*p < 0.05$; $^{†}p < 0.01$; ($*,^{†}$Bonferroni's post hoc test of two-way RM ANOVA). pSTR, positive scotopic threshold responses

a. pSTR response

b. Scotopic b-wave response

c. Scotopic a-wave response
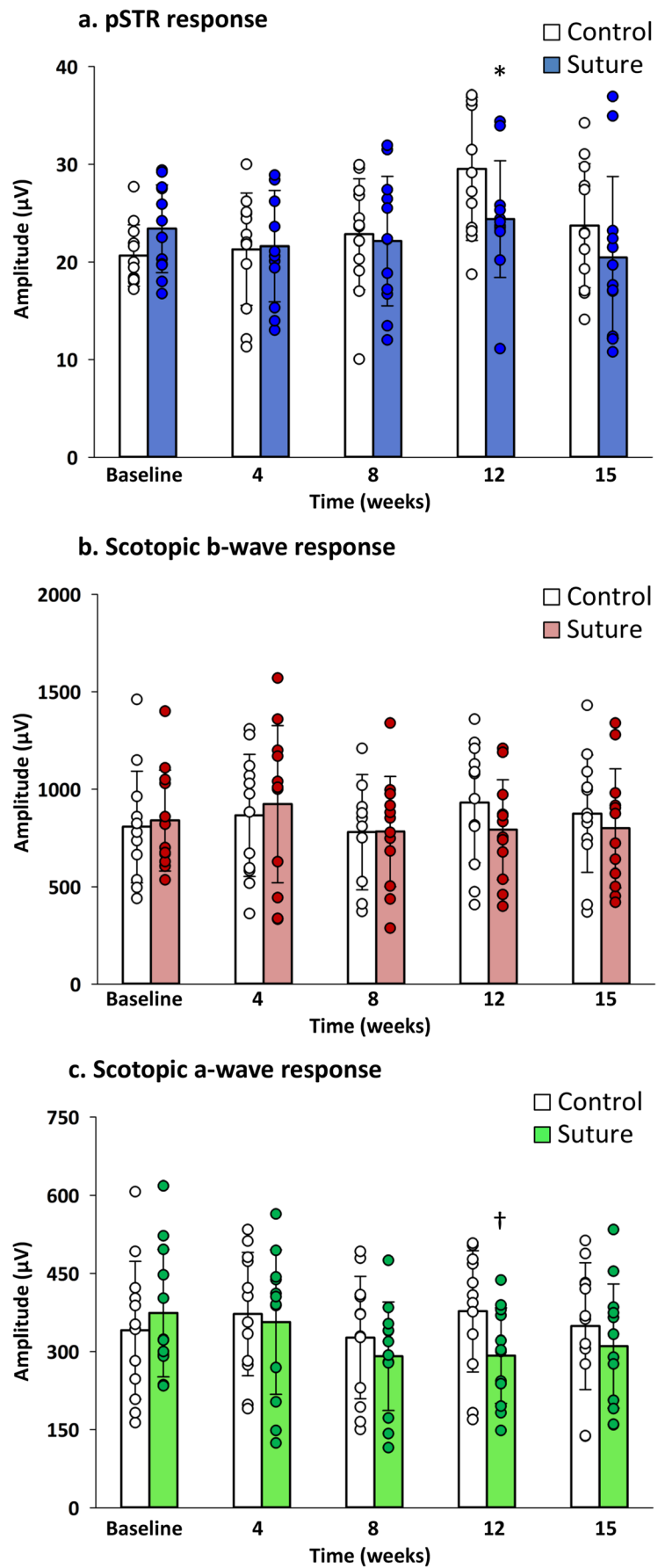
Table 1 Implicit time of pSTR, scotopic b-wave, and a-wave responses of the control and suture eyes measured over 15 weeks

Implicit time (ms)	Eye	Baseline	Week 4	Week 8	Week 12	Week 15
pSTR (SEM)	Control	113.2 (2.7)	114.9 (3.4)	110.7 (1.8)	110.5 (2.7)	117.4 (2.4)
	Suture	114.2 (2.7)	115.1 (3.0)	113.9 (3.2)	113.7 (2.6)	119.3 (2.0)
b-wave (SEM)	Control	69.9 (2.0)	70.4 (1.9)	69.9 (2.4)	78.3 (4.5)	73.0 (1.9)
	Suture	73.2 (2.2)	73.2 (2.6)	74.2 (2.1)*	79.5 (3.1)	73.0 (2.3)
a-wave (SEM)	Control	8.0 (0.1)	7.8 (0.1)	7.7 (0.1)	7.8 (0.4)	7.7 (0.1)
	Suture	7.9 (0.1)	8.1 (0.1)	7.8 (0.1)	8.2 (0.3)†	7.9 (0.1)

*$p < 0.05$

†$p < 0.01$ (*,† Bonferroni's post hoc test of two-way RM ANOVA)

eyes ($-32 \pm 25\%$, $p = 0.02$) as compared with the fellow control eyes (Fig. 8b). Sutured eyes also showed evidence of disruption of axonal bundle organisation with cellular infiltrates in the optic nerve and posterior deformation of optic nerve head surface as compared with fellow control eyes (Fig. 9).

Discussion

This study demonstrated that a circumlimbal suture model produced a moderate, sustained IOP elevation in albino SD rats. The magnitude of IOP elevation in sutured eyes ($\sim 50\%$) was milder than pigmented Long-Evans rat reported in a previous study [19] in which IOP elevation was $\sim 100\%$ above control eyes in the first 4 weeks, gradually dropping to $\sim 60\%$ at week 15. A similar procedure in albino CD-1 mice [32] induced only a milder IOP elevation of ($\sim 30\%$) that sustained for a maximum period of 2 weeks as compared with pigmented C57 mice ($\sim 70\%$) lasting for a period of 12 weeks [22]. The magnitude of IOP elevation following suture implantation appears to be relatively lower in albino strains than

that in the pigmented ones. To ensure that IOP measurements in the present study were not affected by any corneal changes induced by circumlimbal suture, we showed that IOP readings with the rebound tonometer were in good correlation with manometric IOP measurements in sutured SD rat eyes ($n = 5$) (Online Resource 1). Consistent with the previous study [19], no structural differences between the anterior chamber angles of sutured and control eyes were detected in this study (Online Resource 2). These findings suggested that the circumlimbal suture model produced a moderate, chronic elevation of IOP in SD rats, without any observable structural changes in the anterior chamber angles.

On longitudinal evaluation, IOP elevation in albino SD rats produced a significant RNFL thinning as early as week 4 and a corresponding decrease in pSTR response at week 12. As both eyes received the initial IOP spike, the changes in the retinal structure and function quantified in the experimental eyes with respect to control eyes were mainly driven by cumulative IOP over 15 weeks but not by the initial IOP spike. With regard to structure-function relationship, SD rats developed an early RNFL thinning (week 4) that did not progress beyond week 8, whereas pSTR amplitude continued to decline from week 8
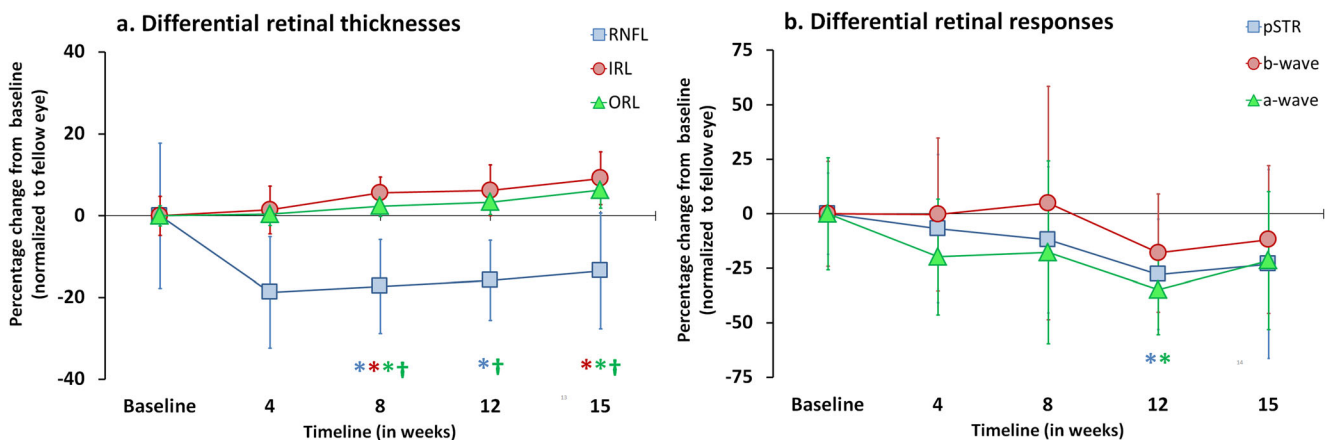
Fig. 6 The effect of chronic IOP on retinal structure and function was summarised as percentage change from fellow control eyes. **a** Thicknesses of RNFL (retinal nerve fibre layer), IRL (inner retinal layer), and ORL (outer retinal layer) measured by OCT and **b** their complementary functional measurements, pSTR (positive scotopic threshold responses), scotopic b-wave, and a-wave responses determined by ERG. Error bars: standard deviation. *$p < 0.05$ vs. baseline; †$p < 0.05$ vs. week 4 (*,† Bonferroni's post hoc test of RM ANOVA)
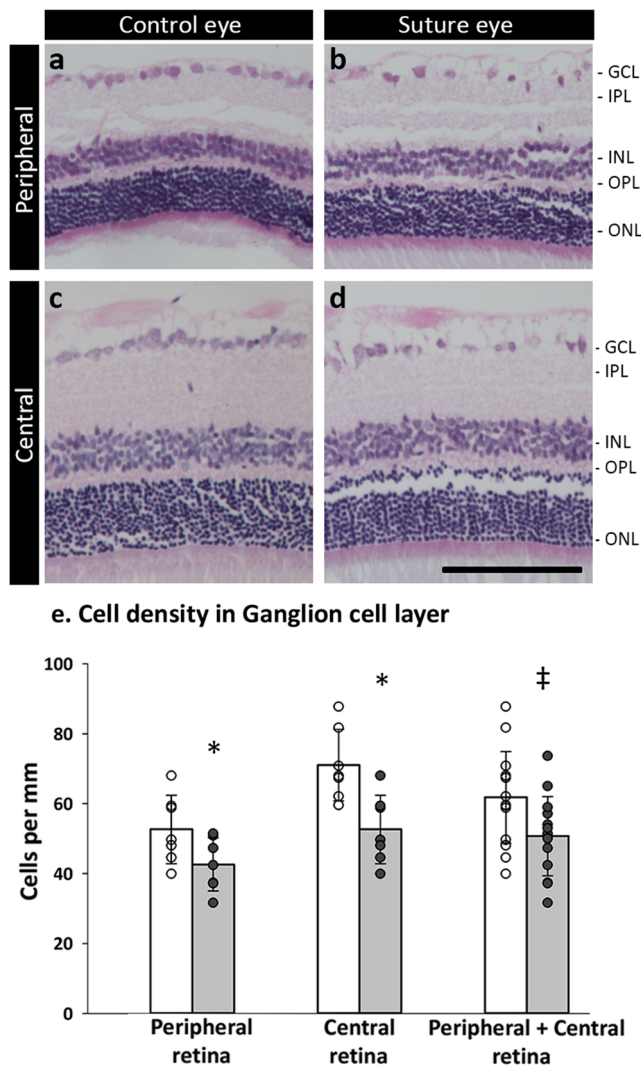
Fig. 7 Effect of chronic IOP on retinal histology and ganglion cell layer density evaluated after 15 weeks of IOP elevation. **a**–**d** Haematoxylin and eosin-stained retinal sections of a representative a, c fellow control and b, d suture eyes in the peripheral (a, b) and central retina (c, d). **e** Cell density in the GCL (cells/mm) in the peripheral retina, central retina, and combined cell count (central and peripheral) of sutured and fellow control eyes ($n = 7$). Error bars: standard deviation. Each circle in the bar chart represents individual data points of the animals. *$p < 0.05$, paired t test. Scale bar: 100 μm

to 12. The RNFL thinning that appeared to precede pSTR attenuation could be due to greater inter-animal variability for the ERG results, which make significant changes harder to detect. Alternatively, IOP-induced changes in membrane stretch-sensitive channels (transient receptor potential vanniloid 1 expression) may transiently increase the magnitude of responses from retinal ganglion cells [36, 37], thus increasing the pSTR response [38]. Under similar OHT induction, albino CD-1 mice [32] was also reported to show an early onset of RNFL loss and a severe thinning as compared with pigmented C57BL6/J [22]; however, functional assessment was not undertaken in this strain [32]. On the other hand,

pigmented Long-Evans rats showed an earlier decline in the ganglion cell function (around week 2 to 4) that produced no further loss, but the RNFL exhibited a gradual and progressive thinning (from week 8 to 15). Consistent with RNFL thinning, the sutured eyes of SD rats showed a significant reduction in cell density in the GCL that was comparable with the quantification using RGC-specific biomarker. While the retinal whole mount quantification of RGC was not performed in the present study, earlier studies reported that the RGC density estimated from retinal cross-sections were comparable to the whole mounted retina [39] or H&E-stained GCL cell density [40] in models of optic nerve injury. Elevated IOP-induced changes including altered arrangements of axon bundles and clustered nuclei of cellular infiltrates, which are suggestive of activated microglia [41–43] in the optic nerve and a posterior tissue displacement of the optic nerve head, were observed.

As for TRT, while the sutured eyes showed a mild increase over time, it was thinned in fellow control eyes (week 15: − $8.0 \pm 1\%$) over 15 weeks of experimentation. We also observed a similar trend of thinning in naïve animals (Online Resource 3), thus possibly excluding the role of initial IOP spike in control eye could have resulted in the gradual decrease in TRT. These finding corroborated with our previous study, where there were no differences in OCT-measured retinal thicknesses between eyes receiving 1 day of OHT and the fellow control eyes [35]. Using histological measurements, Chaychi et al. [44] reported a reduction in the thickness of photoreceptoral layer, inner retinal layer (INL, IPL), and RNFL in normal SD rats between P100 (age equivalent to week 8 follow-up in the present study) and P300. Thus, the reduction in thickness in control eyes could be attributed to normal ageing. Using fellow eyes as controls should account for changes due to ageing and biometric changes over time.

Distinct from other suture studies, both outer (from RPE to OPL) and inner retinal layers (from IPL to INL) of OHT eyes showed a mild increase in thickness from week 8 to week 15, which was associated with a- and b-wave loss between weeks 8 and 12 (a-wave: − $35 \pm 21\%$; b-wave: − $18 \pm 27\%$). At week 15, a small rebound was noticed in the ERG components (a-wave: − $21 \pm 32\%$; b-wave: − $12 \pm 34\%$). In pigmented strains, a non-progressive a-wave reduction was observed with no obvious change in ORL thickness [19, 22]. The decrease in a-wave in the present study may have arisen from compromised choroidal blood flow to the outer retina, either directly from IOP elevation or indirectly from suture compressing the scleral and episcleral plexus. Such reductions in a- and b-wave responses have been reported in other experimental OHT models such as laser photocoagulation of episcleral and limbal veins [16] (SD rats: a-wave: − 45%; b-wave: − 35% at week 8) and cauterisation of episcleral veins (Wistar rats: a-wave: − 30%; b-wave: − 25% at week 8) [24, 45]. Also, a gradual and progressive reduction in the a-wave (7 months of age) followed by b-wave attenuation (8–

Fig. 8 β-III-tubulin labelling of RGC after 15 weeks of IOP elevation. **a** Immunofluorescent staining with anti-β-III-tubulin and DAPI nuclear counterstained retinal sections of a representative control and suture eye at week 15. **b** The RGC density (cells/mm) in the central retina of the control and sutured eyes ($n = 6$). Error bars: standard deviation. Each circle in the bar chart represents individual data points of the animals. $*p < 0.05$, paired t test. Scale bar: 100 μm
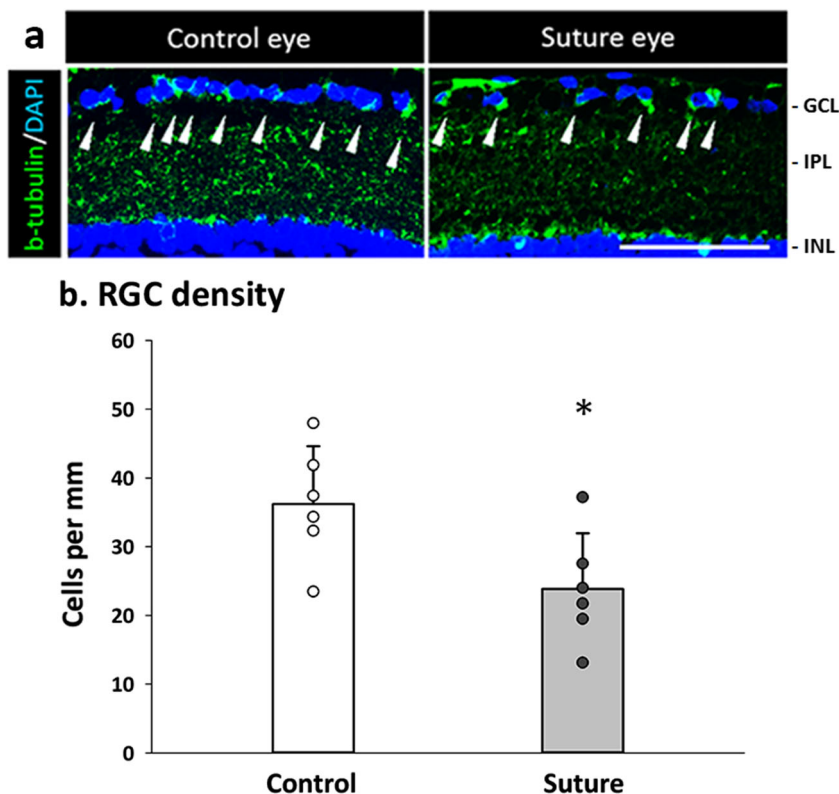
9 months of age) has been also reported in the DBA/2NNia glaucoma model [46]. This outer retinal deficit is thought to arise from reduction in choroidal blood flow, which was detectable at 4 months of age in DBA/2J mice, whereas retinal blood flow deficits were not noted until 6–9 months of age [47]. Previous report showed that suture implantation in C57

Fig. 9 Effect of chronic IOP on the optic nerve morphology evaluated after 15 weeks of IOP elevation. The longitudinal sections of ON were stained with H&E to assess the structural alterations in axonal bundles. Suture eyes with chronic IOP elevation (right column) resulted in posterior deformation of the optic nerve head surface (*). While the cell nuclei are lined up parallel to the axonal bundles in the control optic nerve (left column), such arrangements appear altered in the sutured eyes with clustered nuclei of cellular infiltrates (arrows), which are suggestive of activated microglia. Scale bar: 100 μm
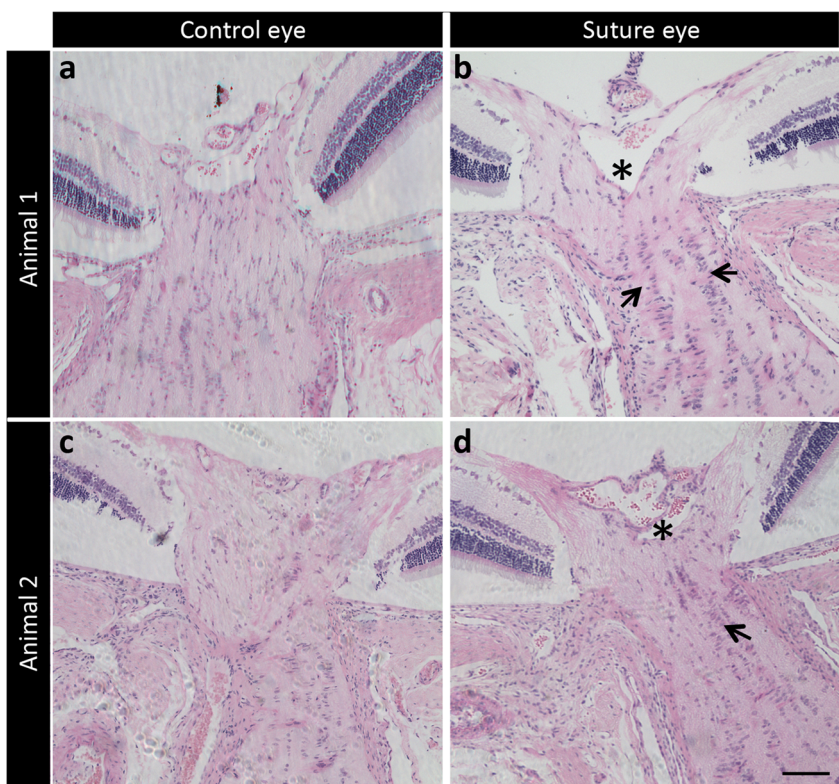
mice for 12 weeks did not cause any change in retinal blood flow (OCT Doppler) [23]. Considering the decrease in scotopic response and the change in ORL thickness in the present study, further investigations are warranted to investigate the possible role of ischemia with circumlimbal suture placement in SD rats. On the other hand, photoreceptoral swelling has been reported previously in human glaucoma (post-mortem donor eyes) and in non-human primate model [48]. Furthermore, Choi et al. [49] showed a loss in cone density among glaucoma subjects of varying severity when imaged using adaptive optics. While the outer retinal changes in glaucoma remains largely equivocal, an underlying secondary vascular cause could possibly be overlooked. Interestingly, Wilsey et al. [50] also reported a thickening of the outer retinal complex ($\sim$ 4 to 5%) in non-human primate experimental glaucoma model (laser photocoagulation of TM) measured by OCT. Consistent with these findings, the present study also observed a relative increase in ORLT from week 8 (2 ± 1%) to week 15 (6 ± 1%), possibly arising from changes in the photoreceptor layer following IOP elevation. However, this interpretation warrants thorough investigation.

It is worth noting that IOP elevation can alter axial length, which in turn affects the OCT measurements of retinal thicknesses (scan position and lateral magnification) [51]. We estimated the eyeball length from a subset of animals ($n = 6$) after collecting the sample for histology. Sutured eyes showed an increase in eyeball length of 0.5 mm (7 ± 3%) as compared with control eyes (Online Resource 4). An increase in axial length should result in a thinner retinal layer. However, the present study found TRT thickening (in particular ORL and IRL) and RNFL thinning. We speculate that the thickening of ORL may arise from compromised choroidal blood circulation, whereas IRL thickening may be related to glial cell proliferation [50, 52, 53].

The effect of suture-induced chronic IOP on retinal structure (RNFL thickness, RGC density) and function (pSTR) reported in pigmented rodent strains [19, 22] was also observed in the present study using SD rats. However, there appears to be a difference in the magnitude of IOP elevation and rate of structural and functional loss between strains. While adherence to surgical protocols and surgeon skills may likely affect the IOP induction, the present study adapted nearly all the surgical recommendations of suture model and was performed by a trained surgeon. In this study, the distance of suture placement (2 mm from limbus) adapted was different from previous reports (1.5 mm from limbus) [19]. During our initial trials of model induction, sutures secured at a distance of 1.5 mm in SD rats were found to slip gradually towards the limbus over time, which could be attributed to the normal age-related increase in eyeball size in addition to the pressure exerted by the suture. This led to sudden IOP spikes and/or the development of corneal changes like steep cornea, cornea vascularisation, and opacity. All these adverse effects were subsequently reduced by securing the suture at a distance of 2 mm from the limbus. We further estimated the suture distance from limbus (SDL) posthumously for a subset of animals ($n = 6$). The SDL did not influence the cumulative IOP ($r = 0.32$; $p = 0.53$); however, it was inversely correlating with the ORLT ($r = -0.84$, $p = 0.04$) (Online Resource 5). As the SDL increased, the ORLT showed less thickening when compared with the control eyes, indicating that the choice of initial suture fixing distance at 2 mm away from limbus was less likely to induce outer retinal changes. However, the suture-encircling procedure, irrespective of suture placement distance, might still have influenced the choroidal blood supply as well as the outer retinal structure and function. The RNFL was not showing progressive thinning in SD rats despite a significant loss at week 4. This may be due to the activation of glial cells, often detected during the process of neurodegeneration, masking the thinning of RNFL at later time points of the disease course [52, 54]. Also, the magnitude of IOP elevation in the earlier weeks ($\sim$ 50% elevation) was not subsequently maintained in the later period ($\sim$ 25% elevation from week 4 to 12), which could possibly lower the rate of RNFL thinning after week 4. Although the current study did not use other strains, an earlier study reported a strain-specific difference in which albino mice (CD-1) manifested greater axonal and RGC loss following intracameral microbead injection as compared with other two pigmented mouse strains (C57, DBA/2J), despite all groups developed similar magnitudes of IOP elevation [10]. Moreover, Bakalash et al. [55] reported a difference in susceptibility between two albino strains in which Lewis rat developed relatively greater RGC loss than SD rats when IOP was chronically elevated by laser photocoagulation of episcleral and limbal veins. The degree of IOP elevation and neuronal vulnerability between strains may be influenced by aqueous humour dynamics [56], scleral biomechanical properties [57], or immunological background [55, 58] of different rodent strains. Thus strain-specific neuronal susceptibility to stress [10, 59–62] should be taken into account when comparing between studies. Besides, such differences between strains are in line with clinical scenario wherein patient responds distinctly to IOP stress (while some show resistance to IOP elevation, others are vulnerable to normal IOP levels) or progress at different rates to IOP elevation (while some progress at slower rate, others develop faster disease progression). Therefore, strain-specific neuronal susceptibility can be advantageously utilised as models simulating various clinical conditions to study the disease pathogenesis and to test the efficacy of neuroprotective agents at the level of preclinical research [35, 63].

In summary, following a single intervention, the circumlimbal suture OHT model in albino SD rats produced a moderate chronic IOP elevation that resulted in RNFL thinning and RGC loss. Also, the retinal function declined gradually over time, thus providing a time window to test the effects

of anti-glaucoma drugs, for example, the neuroprotective agents. However, SD rats also developed a small increase in both inner and outer retinal thicknesses. Over the course of the 15-week experimentation, it was important to take into account age-related thinning of retinal layers. As the onset and the rate of structural and functional changes observed using SD rats differed from earlier reports using pigmented strain, comparisons with other studies should take into account for strain-specific differences.

Compliance with ethical standards

Conflict of interest The authors declare that they have no conflict of interest.

Ethical approval All applicable international, national, and/or institutional guidelines for the care and use of animals were followed.

References

1. Tham YC, Li X, Wong TY, Quigley HA, Aung T, Cheng CY (2014) Global prevalence of glaucoma and projections of glaucoma burden through 2040: a systematic review and meta-analysis. Ophthalmology 121(11):2081–2090. https://doi.org/10.1016/j.ophtha.2014.05.013

2. Quigley HA, Broman AT (2006) The number of people with glaucoma worldwide in 2010 and 2020. Br J Ophthalmol 90(3):262–267. https://doi.org/10.1136/bjo.2005.081224

3. Heijl A, Leske MC, Bengtsson B, Hyman L, Bengtsson B, Hussein M, Early Manifest Glaucoma Trial G (2002) Reduction of intraocular pressure and glaucoma progression: results from the early manifest glaucoma trial. Arch Ophthalmol 120(10):1268–1279. https://doi.org/10.1001/archopht.120.10.1268

4. Kass MA, Heuer DK, Higginbotham EJ, Johnson CA, Keltner JL, Miller JP, Parrish RK, Wilson MR, Gordon MO (2002) The ocular hypertension treatment study: a randomized trial determines that topical ocular hypotensive medication delays or prevents the onset of primary open-angle glaucoma. Arch Ophthalmol 120(6):701–713

5. Group CN-TGS (1998) Comparison of glaucomatous progression between untreated patients with normal-tension glaucoma and patients with therapeutically reduced intraocular pressures. Am J Ophthalmol 126(4):487–497

6. Bouhenni R, Dunmire J, Sewell A, Edward DP (2012) Animal models of glaucoma. Biomed Res Int 2012:692609. https://doi.org/10.1155/2012/692609

7. Johnson TV, Tomarev SI (2010) Rodent models of glaucoma. Brain Res Bull 81(2–3):349–358

8. Vecino E, Sharma SC (2011) Glaucoma animal models. In: Glaucoma-Basic and Clinical Concepts. IntechOpen, pp 319–334

9. Urcola JH, Hernández M, Vecino E (2006) Three experimental glaucoma models in rats: comparison of the effects of intraocular pressure elevation on retinal ganglion cell size and death. Exp Eye Res 83(2):429–437

10. Cone FE, Gelman SE, Son JL, Pease ME, Quigley HA (2010) Differential susceptibility to experimental glaucoma among 3 mouse strains using bead and viscoelastic injection. Exp Eye Res 91(3):415–424

11. Sappington RM, Carlson BJ, Crish SD, Calkins DJ (2010) The microbead occlusion model: a paradigm for induced ocular hypertension in rats and mice. Invest Ophthalmol Vis Sci 51(1):207–216

12. Levkovitch-Verbin H, Quigley HA, Martin KR, Valenta D, Baumrind LA, Pease ME (2002) Translimbal laser photocoagulation to the trabecular meshwork as a model of glaucoma in rats. Invest Ophthalmol Vis Sci 43(2):402–410

13. Biermann J, van Oterendorp C, Stoykow C, Volz C, Jehle T, Boehringer D, Lagrèze WA (2012) Evaluation of intraocular pressure elevation in a modified laser-induced glaucoma rat model. Exp Eye Res 104:7–14

14. Ueda J, Sawaguchi S, Hanyu T, Yaoeda K, Fukuchi T, Abe H, Ozawa H (1998) Experimental glaucoma model in the rat induced by laser trabecular photocoagulation after an intracameral injection of India ink. Jpn J Ophthalmol 42(5):337–344

15. WoldeMussie E, Ruiz G, Wijono M, Wheeler LA (2001) Neuroprotection of retinal ganglion cells by brimonidine in rats with laser-induced chronic ocular hypertension. Invest Ophthalmol Vis Sci 42(12):2849–2855

16. Li RS, Tay DK, Chan HH, So KF (2006) Changes of retinal functions following the induction of ocular hypertension in rats using argon laser photocoagulation. Clin Exp Ophthalmol 34(6):575–583

17. Morrison JC, Moore C, Deppmeier LM, Gold BG, Meshul CK, Johnson EC (1997) A rat model of chronic pressure-induced optic nerve damage. Exp Eye Res 64(1):85–96

18. Shareef S, Garcia-Valenzuela E, Salierno A, Walsh J, Sharma S (1995) Chronic ocular hypertension following episcleral venous occlusion in rats. Exp Eye Res 61(3):379–382

19. Liu H-H, Bui BV, Nguyen CT, Kezic JM, Vingrys AJ, He Z (2015) Chronic ocular hypertension induced by circumlimbal suture in rats. Invest Ophthalmol Vis Sci 56(5):2811–2820

20. Liu HH, He Z, Nguyen CT, Vingrys AJ, Bui BV (2017) Reversal of functional loss in a rat model of chronic intraocular pressure elevation. Ophthalmic Physiol Opt 37(1):71–81

21. Zhao D, Wong VHY, He Z, Nguyen CTO, Jobling AI, Fletcher E, Chinnery H, Jusuf P, Lim JK, Vingrys AJ (2018) Reversibility of retinal ganglion cell dysfunction due to chronic IOP elevation. Invest Ophthalmol Vis Sci 59(9):3696–3696

22. Liu H-H, Flanagan JG (2017) A mouse model of chronic ocular hypertension induced by circumlimbal suture. Invest Ophthalmol Vis Sci 58(1):353–361

23. Zhao D, Nguyen CT, Wong VH, Lim JK, He Z, Jobling AI, Fletcher EL, Chinnery HR, Vingrys AJ, Bui BV (2017) Characterization of the circumlimbal suture model of chronic IOP elevation in mice and assessment of changes in gene expression of stretch sensitive channels. Front Neurosci 11:41

24. Bayer AU, Danias J, Brodie S, Maag KP, Chen B, Shen F, Podos SM, Mittag TW (2001) Electroretinographic abnormalities in a rat glaucoma model with chronic elevated intraocular pressure. Exp Eye Res 72(6):667–677. https://doi.org/10.1006/exer.2001.1004

25. Ben-Shlomo G, Bakalash S, Lambrou GN, Latour E, Dawson WW, Schwartz M, Ofri R (2005) Pattern electroretinography in a rat model of ocular hypertension: functional evidence for early

detection of inner retinal damage. Exp Eye Res 81(3):340–349. https://doi.org/10.1016/j.exer.2005.02.006

26. Kim DH, Kim HS, Ahn MD, Chun MH (2004) Ganglion cell death in rat retina by persistent intraocular pressure elevation. Korean J Ophthalmol 18(1):15–22. https://doi.org/10.3341/kjo.2004.18.1.15

27. Chan HC, Chang RC, Koon-Ching Ip A, Chiu K, Yuen WH, Zee SY, So KF (2007) Neuroprotective effects of Lycium barbarum Lynn on protecting retinal ganglion cells in an ocular hypertension model of glaucoma. Exp Neurol 203(1):269–273. https://doi.org/10.1016/j.expneurol.2006.05.031

28. Colafrancesco V, Parisi V, Sposato V, Rossi S, Russo MA, Coassin M, Lambiase A, Aloe L (2011) Ocular application of nerve growth factor protects degenerating retinal ganglion cells in a rat model of glaucoma. J Glaucoma 20(2):100–108. https://doi.org/10.1097/IJG.0b013e3181d787e5

29. Hernández M, Urcola JH, Vecino E (2008) Retinal ganglion cell neuroprotection in a rat model of glaucoma following brimonidine, latanoprost or combined treatments. Exp Eye Res 86(5):798–806. https://doi.org/10.1016/j.exer.2008.02.008

30. Sarup V, McEwan GC, Thompson C, Patil KA, Sharma SC (2005) Dorzolamide and timolol saves retinal ganglion cells in glaucomatous adult rats. J Ocul Pharmacol Ther 21(6):454–462. https://doi.org/10.1089/jop.2005.21.454

31. Seki M, Tanaka T, Matsuda H, Togano T, Hashimoto K, Ueda J, Fukuchi T, Abe H (2005) Topically administered timolol and dorzolamide reduce intraocular pressure and protect retinal ganglion cells in a rat experimental glaucoma model. Br J Ophthalmol 89(4):504–507. https://doi.org/10.1136/bjo.2004.052860

32. Liu H-H, Zhang L, Shi M, Chen L, Flanagan JG (2017) Comparison of laser and circumlimbal suture induced elevation of intraocular pressure in albino CD-1 mice. PLoS One 12(11): e0189094

33. Lakshmanan Y, Wong FS, Yu WY, Li SZ, Choi KY, So KF, Chan HH (2019) Lycium Barbarum polysaccharides rescue neurodegeneration in an acute ocular hypertension rat model under pre- and posttreatment conditions. Invest Ophthalmol Vis Sci 60(6):2023–2033. https://doi.org/10.1167/iovs.19-26752

34. Bui BV, Fortune B (2004) Ganglion cell contributions to the rat full-field electroretinogram. J Physiol 555(1):153–173

35. Lakshmanan Y, Wong FSY, Zuo B, So K-F, Bui BV, Chan HH-L (2019) Posttreatment intervention with Lycium Barbarum polysaccharides is neuroprotective in a rat model of chronic ocular hypertension. Invest Ophthalmol Vis Sci 60(14):4606–4618. https://doi.org/10.1167/iovs.19-27886

36. Weitlauf C, Ward NJ, Lambert WS, Sidorova TN, Ho KW, Sappington RM, Calkins DJ (2014) Short-term increases in transient receptor potential vanilloid-1 mediate stress-induced enhancement of neuronal excitation. J Neurosci 34(46):15369–15381

37. Risner ML, Pasini S, Cooper ML, Lambert WS, Calkins DJ (2018) Axogenic mechanism enhances retinal ganglion cell excitability during early progression in glaucoma. Proc Natl Acad Sci 115(10):E2393–E2402

38. Choh V, Gurdita A, Tan B, Prasad RC, Bizheva K, Joos KM (2016) Short-term moderately elevated intraocular pressure is associated with elevated scotopic electroretinogram responses. Invest Ophthalmol Vis Sci 57(4):2140–2151

39. Mead B, Thompson A, Scheven BA, Logan A, Berry M, Leadbeater W (2014) Comparative evaluation of methods for estimating retinal ganglion cell loss in retinal sections and wholemounts. PLoS One 9(10):e110612. https://doi.org/10.1371/journal.pone.0110612

40. Dheer Y, Chitranshi N, Gupta V, Sharma S, Pushpitha K, Abbasi M, Mirzaei M, You Y, Graham SL, Gupta V (2019) Retinoid x receptor modulation protects against ER stress response and rescues glaucoma phenotypes in adult mice. Exp Neurol 314:111–125. https://doi.org/10.1016/j.expneurol.2019.01.015

41. Shindler KS, Guan Y, Ventura E, Bennett J, Rostami A (2006) Retinal ganglion cell loss induced by acute optic neuritis in a relapsing model of multiple sclerosis. Mult Scler J 12(5):526–532. https://doi.org/10.1177/1352458506070629

42. Horstmann L, Schmid H, Heinen AP, Kurschus FC, Dick HB, Joachim SC (2013) Inflammatory demyelination induces glia alterations and ganglion cell loss in the retina of an experimental autoimmune encephalomyelitis model. J Neuroinflammation 10:120–120. https://doi.org/10.1186/1742-2094-10-120

43. Renner M, Stute G, Alzureiqi M, Reinhard J, Wiemann S, Schmid H, Faissner A, Dick HB, Joachim SC (2017) Optic nerve degeneration after retinal ischemia/reperfusion in a rodent model. Front Cell Neurosci 11:254–254. https://doi.org/10.3389/fncel.2017.00254

44. Chaychi S, Polosa A, Lachapelle P (2015) Differences in retinal structure and function between aging male and female Sprague-Dawley rats are strongly influenced by the estrus cycle. PLoS One 10(8):e0136056

45. Mittag TW, Danias J, Pohorenec G, Yuan HM, Burakgazi E, Chalmers-Redman R, Podos SM, Tatton WG (2000) Retinal damage after 3 to 4 months of elevated intraocular pressure in a rat glaucoma model. Invest Ophthalmol Vis Sci 41(11):3451–3459

46. Bayer AU, Neuhardt T, May AC, Martus P, Maag K-P, Brodie S, Lütjen-Drecoll E, Podos SM, Mittag T (2001) Retinal morphology and ERG response in the DBA/2NNia mouse model of angle-closure glaucoma. Invest Ophthalmol Vis Sci 42(6):1258–1265

47. Lavery WJ, Muir ER, Kiel JW, Duong TQ (2012) Magnetic resonance imaging indicates decreased choroidal and retinal blood flow in the DBA/2J mouse model of glaucoma. Invest Ophthalmol Vis Sci 53(2):560–564

48. Nork TM, Ver Hoeve JN, Poulsen GL, Nickells RW, Davis MD, Weber AJ, Sarks SH, Lemley HL, Millecchia LL (2000) Swelling and loss of photoreceptors in chronic human and experimental glaucomas. Arch Ophthalmol 118(2):235–245

49. Choi SS, Zawadzki RJ, Lim MC, Brandt JD, Keltner JL, Doble N, Werner JS (2011) Evidence of outer retinal changes in glaucoma patients as revealed by ultrahigh-resolution in vivo retinal imaging. Br J Ophthalmol 95(1):131–141

50. Wilsey LJ, Reynaud J, Cull G, Burgoyne CF, Fortune B (2016) Macular structure and function in nonhuman primate experimental glaucoma. Invest Ophthalmol Vis Sci 57(4):1892–1900

51. Lozano DC, Twa MD (2013) Development of a rat schematic eye from in vivo biometry and the correction of lateral magnification in SD-OCT imaging. Invest Ophthalmol Vis Sci 54(9):6446–6455

52. Hood DC, Lin CE, Lazow MA, Locke KG, Zhang X, Birch DG (2009) Thickness of receptor and post-receptor retinal layers in patients with retinitis pigmentosa measured with frequency-domain optical coherence tomography. Invest Ophthalmol Vis Sci 50(5):2328–2336

53. Kim EK, Park H-YL, Park CK (2017) Relationship between retinal inner nuclear layer thickness and severity of visual field loss in glaucoma. Sci Rep 7(1):5543

54. Choe TE, Abbott CJ, Piper C, Wang L, Fortune B (2014) Comparison of longitudinal in vivo measurements of retinal nerve fiber layer thickness and retinal ganglion cell density after optic nerve transection in rat. PLoS One 9(11):e113011. https://doi.org/10.1371/journal.pone.0113011

55. Bakalash S, Kipnis J, Yoles E, Schwartz M (2002) Resistance of retinal ganglion cells to an increase in intraocular pressure is immune-dependent. Invest Ophthalmol Vis Sci 43(8):2648–2653

56. Boussommier-Calleja A, Overby DR (2013) The influence of genetic background on conventional outflow facility in mice Strain-Dependent Conventional Outflow facility in mice. Invest Ophthalmol Vis Sci 54(13):8251–8258. https://doi.org/10.1167/iovs.13-13025

57. Nguyen C, Cone FE, Nguyen TD, Coudrillier B, Pease ME, Steinhart MR, Oglesby EN, Jefferys JL, Quigley HA (2013)

Studies of scleral biomechanical behavior related to susceptibility for retinal ganglion cell loss in experimental mouse glaucoma Scleral Biomechanical Behavior in Mouse Glaucoma. Invest Ophthalmol Vis Sci 54(3):1767–1780. https://doi.org/10.1167/iovs.12-10952

58. Huang Y, Li Z, van Rooijen N, Wang N, Pang CP, Cui Q (2007) Different responses of macrophages in retinal ganglion cell survival after acute ocular hypertension in rats with different autoimmune backgrounds. Exp Eye Res 85(5):659–666. https://doi.org/10.1016/j.exer.2007.07.020

59. Dorfman AL, Polosa A, Joly S, Chemtob S, Lachapelle P (2009) Functional and structural changes resulting from strain differences in the rat model of oxygen-induced retinopathy. Invest Ophthalmol Vis Sci 50(5):2436–2450

60. Gurdita A, Tan B, Joos KM, Bizheva K, Choh V (2017) Pigmented and albino rats differ in their responses to moderate, acute and reversible intraocular pressure elevation. Doc Ophthalmol 134(3):205–219. https://doi.org/10.1007/s10633-017-9586-x

61. Polosa A, Bessaklia H, Lachapelle P (2016) Strain differences in light-induced retinopathy. PLoS One 11(6):e0158082

62. Safa R, Osborne NN (2000) Retinas from albino rats are more susceptible to ischaemic damage than age-matched pigmented animals. Brain Res 862(1–2):36–42

63. Livne-Bar I, Wei J, Liu H-H, Alqawlaq S, Won G-J, Tuccitto A, Gronert K, Flanagan JG, Sivak JM (2017) Astrocyte-derived lipoxins A 4 and B 4 promote neuroprotection from acute and chronic injury. J Clin Invest 127(12):4403–4414